Historical changes in drought characteristics and its impact on vegetation cover over Madagascar

Herijaona Hani-Roge Hundilida Randriatsara[1], Eva Holtanova[1], Karim Rizwan[2], Hassen Babaousmail[3], Mirindra Finaritra Tanteliniaina Rabezanahary[4], Kokou Romaric Posset[5], Donnata Alupot[6], Brian Odhiambo Ayugi[7]

[1]Department of Atmospheric Physics, Faculty of Mathematics and Physics, Charles University, Prague, V Holešovičkách 2, 18000, Prague 8, Czech Republic
[2]Key Laboratory of Meteorological Disaster, Ministry of Education (KLME)/Joint International Research Laboratory of Climate and Environment Change (ILCEC)/Collaborative Innovation Center on Forecast and Evaluation of Meteorological Disasters (CIC-FEMD), Nanjing, University of Information Science and Technology, Nanjing 210044, China
[3]School of Atmospheric Science and Remote Sensing, Wuxi University, Wuxi 214105, China
[4]Responsible people acting for development, Antananarivo 101, Madagascar
[5]Climate Change Department, Pan African University Institute for Water and Energy Sciences (Including Climate Change), C/O Université Abou Bekr Belkaid Tlemcen, Campus Chetouane, Tlemcen, Algeria
[6]Uganda National Meteorological Authority, plot 21, 28 portbell road Luzira-Kampala, P.O.Box 7025
[7]Department of Civil Engineering, Seoul National University of Science and Technology, Seoul 01811, Republic of Korea

Correspondence to: Herijaona Hani-Roge Hundilida Randriatsara (hundilida.randriatsara@matfyz.cuni.cz)

Abstract. Drought has become one of the most devastating natural hazards in recent decades causing severe vegetation degradation. This study aims to analyze the spatiotemporal characteristics of drought (duration, frequency, severity, intensity) over Madagascar during 1981-2022. In addition, it evaluates the relationship between the Standardized Precipitation Index (SPI) and the Normalized Difference Vegetation Index (NDVI) during 2000-2022, representing the impact of drought on vegetation over the studied area. Drought assessment was computed on SPI-3, SPI-6, and SPI-12 timescales, accompanied by seasonal and annual analyses. While the NDVI-SPI relationships were performed through the analysis of vegetation changes based on specific selected SPI time-periods and the correlation analysis. The findings reveal that drought events have become more consecutive during the most recent past (2017 to 2022) and intensified over the southern part of the country. Links between the drought occurrence and vegetation changes are confirmed: the occurrences of continuous negative values of seasonal and annual SPI increase vegetation losses, and the existence of smaller negative values of the wet season SPI relates to more vegetation degradation during the wet season. The correlation between NDVI anomaly and SPI emphasizes the NDVI-SPI relationship found with statistical significance, especially over southern Madagascar. These findings are crucial for complementing other climatic factors that influence Madagascar's vegetation besides drought.

1 Introduction

Drought has been identified as one of the gravest natural disasters experienced across the planet (Wilhite, 2000; Kalisa et al., 2020). Research has shown that droughts are some of the most damaging natural hazards, deteriorating means of living, including vegetation, due to its significant impacts on diverse sectors (Gouveia et al., 2017; Mbatha and Sifiso, 2018; Kannenberg et al., 2020; Lawal et al., 2021). Droughts are present across various climatic regions, including those with high and low precipitation levels, and are primarily linked to a prolonged decrease in rainfall over a specific period, such as a season or a year (Mishra and Singh, 2010). Drought event can be categorized as; meteorological drought, caused by insufficient rainfall during a specific timeframe; hydrological drought, linked to the inadequate surface and groundwater availability; agricultural drought, resulting from a scarcity of water for plant growth; and socio-economic drought, which pertains to an inadequate supply to meet the demand for various economic commodities, encompassing the aforementioned three types of droughts (Heim, 2002; Udmale et al., 2014). According to the Intergovernmental Panel on Climate Change (IPCC), global droughts are projected to intensify and occur more frequently worldwide due to climate change (IPCC, 2021).

For the case of Madagascar, fewer studies have assessed drought events. Desbureaux and Damania (2018) assessed the impact of drought in inducing deforestation and degradation of biodiversity conservation over the country using the SPI method. However, the study lacks in-depth analysis of drought characteristics such as its frequency, its duration, its intensity, and its spatial patterns. As well as, Randriamarolaza et al. (2021) studied spatio-temporal drought characteristics in terms of its magnitude and duration only by using the SPEI method. Moreover, their study presents some limitations such as the use of fewer station data that represent numerous missing values, and the dependency on data quality control and homogenization methods to complement these missing values. All of these might lead to some extent of uncertainties in the outputs. However, the Intergovernmental Panel on Climate Change Assessment Reports six (IPCC, 2021) reported that medium confidence level in the drought changes over Madagascar has been projected, mainly attributed to the lack of sufficient evidence. This calls for an urgent need to conduct more in-depth studies over the country to identify the most affected regions by drought in terms of its full characteristics (duration, frequency, severity and intensity).

Vegetation plays a vital role in natural ecosystems by managing the flow of water, carbon, and energy, offering habitats for various organisms, and ensuring global food and water security (Konduri et al., 2022). Droughts are widely recognized to cause diminishing of the primary and secondary productivity of vegetation and forests, triggering, among other negative influences, the occurrence of tree mortality, and the loss of pastures (Smit et al., 2008; Bennett et al., 2015,). Southern Madagascar is currently facing severe food insecurity due to a significant drop in rice, maize, and cassava yields caused by the most severe drought in four decades, accompanied by sandstorms and pest invasions (Narvaez and Eberle, 2022). Studies have indicated that during drought, there is an observed rise in deforestation rates over Madagascar as farmers resort to clearing more forests to counter the adverse effects on agricultural productivity (Desbureaux and Damania, 2018). Assessing how Madagascar's vegetation reacts to drought is crucial for understanding the susceptibility of the ecosystem on the island to extreme climatic events. Analyzing the historical patterns of drought and its effects on vegetation can offer valuable insights

for planning environmental, natural resource, and developmental strategies, pinpointing vulnerable ecosystems and livelihoods at risk of degradation or loss due to heightened drought conditions in the future. Thus, a comprehensive evaluation of the impact of drought events on natural ecosystems will offer insights into recent changes in vegetation to endure water scarcity (Chaves et al., 2003; Kannenberg et al., 2020) and the complex interplay between the severity and duration of droughts in relation to their effects on vegetation (Vicente-Serrano et al., 201; Gouveia et al., 2017).

Choosing the right drought index is fundamental for identifying and defining droughts (Yao et al., 2018). This present study employs Standardized Precipitation Index (SPI) (McKee et al., 1993), not only because it is recommended by the World Meteorological Organization (WMO) to be used for drought analysis (Svoboda and Fuchs, 2017) but also for its simplicity and because many studies have successfully employed it in various regions (Elkollaly et al., 2018; Nkunzimana et al., 2021; Lawal et al., 2021; Nguyễn et al., 2023). To the best of our knowledge, it has not been studied over Madagascar so far. Even though incorporating an index based on soil moisture would be beneficial for analyzing drought impacts on vegetation, SPI is frequently used for studying agricultural droughts since it requires only precipitation data, which has better availability. Besides, an appropriate index describing the vegetation cover must be used to investigate the impact of drought on vegetation. It is reported that the normalized difference vegetation index (NDVI) is the most extensively used vegetation index to investigate climate impacts on vegetation (Tian et al., 2015; Huang et al., 2021). This index has been successfully used and shown as a good indicator of vegetation greenness, biomass, leaf area index, and primary production (Huete et al., 2002; Sun et al., 2011., Mbatha and Sifiso, 2018; Sharma et al., 2022). Out of the numerous vegetation indices, the NDVI is also a reliable measure for tracking vegetation status, commonly employed in monitoring land degradation, desertification, and often utilized for detecting and evaluating drought conditions (Zhao et al., 2018; Nanzad et al., 2019; Lawal et al., 2021). As an illustration, relationships between drought by using SPI method and vegetation indices including NDVI have been successfully evaluated over Africa (Vicente-Serrano et al., 2013; Lawal et al., 2021). However, so far, any similar assessment of drought and its impacts on vegetation has not been performed over Madagascar**.**

Therefore, the aim of the present study is to evaluate the features of drought over Madagascar in recent decades from 1981 to 2022 and to assess the potential impact of selected drought episodes on vegetation. For the characterization of historical drought patterns and its effects on vegetation across Madagascar, this study employs SPI as the drought index and NDVI as the vegetation index. The drought assessment is conducted on multiple SPI timescales accompanied by seasonal and annual analyses. Furthermore, it accounts for detailed examination in drought duration, frequency, severity and intensity. By connecting SPI and NDVI changes, the relationships between precipitation deficits and vegetation response could be explored.

2 Study area, data, and methods

2.1 Study Area

Madagascar is situated in the Indian Ocean, near the southeastern coast of Africa, within the coordinates of 12° - 25°S and 43° - 51°E, covering an area of approximately 592,040 km2 (Fig. 1). The country experiences two primary seasons: a hot-wet

season from November to April and a cool-dry season from May to October (Jury et al., 1995; Randriamarolaza et al., 2021; Randriatsara et al., 2022a). These seasonal variations are primarily influenced by Madagascar's topography and geographical location (Jury et al., 1995; Macron et al., 2016; Randriatsara et al., 2022a; Barimalala et al., 2018). The elevation of the Island reaches up to 2300m in the central highland above the sea level (Fig.1a). Annual rainfall across the country varies from 350 to 4000 mm/year (≃ 30 to 300 mm/month (Fig. 1c)), with a decreasing gradient from the eastern coast to the southwestern coast (Randriatsara et al., 2022a, 2022b and 2023). Daily mean air temperature varies throughout the year from 23 to 27°C (≃ 296 to 303 [K]) in coastal regions and from 14 to 22°C (≃ 287 to 295 [K]) in the central highlands (Fig. 1d). During the hot-wet season, the Inter-Tropical Convergence Zone (ITCZ) covers the northern part of the country as the northwest monsoon wind and the trade winds converge over this area (Randriamarolaza et al., 2021). This convergence leads to rainfall across the whole of Madagascar except the southern parts. In contrast, these semi-arid southern regions receive precipitation when the tropical temperate trough develops between November and February, extending from Southern Africa to the Mozambique Channel (Macron et al., 2016; Barimalala et al., 2018). The southern region has low vegetation cover and a dry steppe climate (Belda et al., 2014). In this study, we divided Madagascar into three regions (Fig. 1) in accordance with the general land characteristics, the amount of rainfall (Fig.1c), the mean temperature (Fig.1d) and the vegetation types. Region 1 (R1) is the southern part of the country, the semi-arid area where the spiny forests reside. Region 2 (R2) is the western part covered by dry forests (i.e., forests that can survive under a low amount of rain), while Region 3 (R3) is the eastern coast and represents the tropical rainforest (Burgess et al., 2004; Desbureaux and Damania, 2018). Moreover, it is worth mentioning that in this study, the borders of the regions are only simple straight lines based on the distribution of annual mean precipitation and temperature over Madagascar. This is done for the sake of simplicity, but the regions are coherent mainly in terms of precipitation, which is the only input for the SPI calculation. Also, prevailing vegetation types are consistent within the three studied regions.

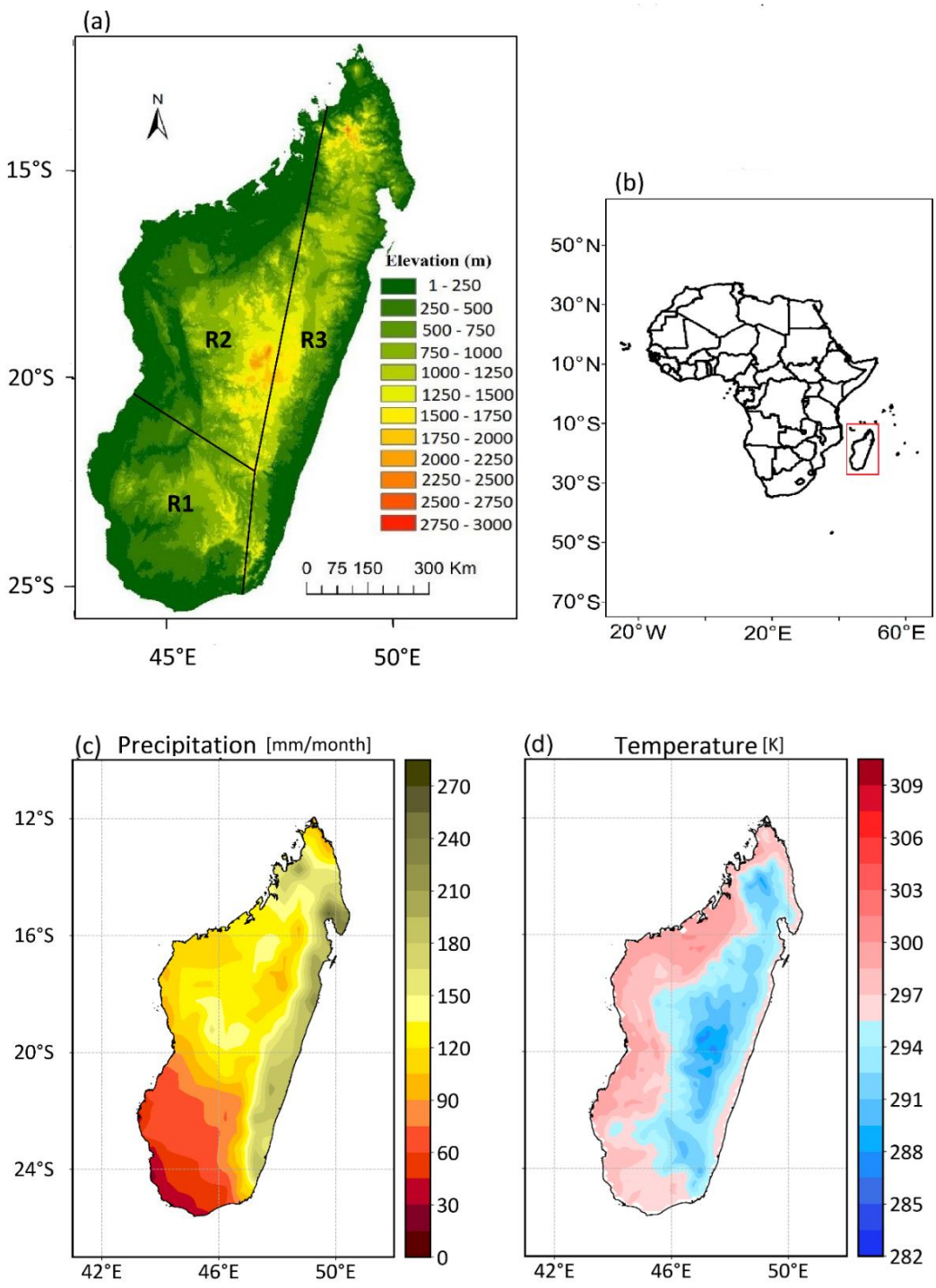

120

Figure 1: (a) Topographic map of the study area. (b) geographical location of Madagascar (depicted in red rectangle) on the Africa map. (c) Precipitation and (d) temperature annual mean of Madagascar from 1981-2022. R1 represents the southern region, R2 the western region and R3 the eastern region.

2.2 Data

2.2.1 Precipitation data

The choice of the datasets for this study is based on the findings from our previous research (Randriatsara et al., 2022b), which evaluated the performance of different gridded (gauge-based, reanalysis and satellite) precipitation datasets over Madagascar during 1983-2015. Among all the examined datasets, CHIRPS v2.0 (Climate Hazards Group InfraRed Precipitation with Station data, version 2.0) and ERA5 (ECMWF Reanalysis v5-Land) were found to best represent Madagascar's rainfall. Moreover, these two datasets have been chosen and successfully used as reference data for evaluating the performance of CMIP6 HighResMIP over Madagascar during 1981-2014 (Randriatsara et al., 2023).

The CHIRPS data is a satellite dataset, derived from infrared cold cloud duration accompanied by smart interpolation technique, covering a wide geographical range from 50°S to 50°N with a spatial resolution of 0.05 × 0.05 (5.3 km) and spanning the period from 1981 to near-present (Funk et al., 2015). Among all the research, it has been successfully used to assess drought characteristics in the Gamo Zone, Ethiopia, and found to perform well (Shalishe et al. (2022). Similarly, Li et al. (2023) demonstrated that CHIRPS effectively reproduced the spatial distribution of drought characteristics in China's first-level water resource basins based on the standardized precipitation index (SPI). It is available at https://iridl.ldeo.columbia.edu/SOURCES/.UCSB/.CHIRPS/.v2p0/.daily-improved/.global/.0p05/.prcp. Besides, the ERA5 data is the fifth-generation atmospheric reanalysis developed by ECMWF, integrates data from over 200 satellite instruments, as well as ground-based radar-gauge data for rainfall (Hersbach et al., 2020). This dataset covers a spatial resolution of about 0.1 × 0.1 over several decades and spans from January 1959 to the near present. Moreover, it has proven valuable in the field of drought analysis (Rakhmatova et al., 2021; Vicente-Serrano et al., 2022) and outperforming over other products in monitoring drought characteristics in South Africa (Tladi et al. 2022). The ERA5 dataset is available at https://cds.climate.copernicus.eu/cdsapp#!/home.

The current study offers the use of combining CHIRPS v2.0 and ERA5 data for a robust and enhanced dataset for the comprehensive analysis of drought characteristics over the study area. Both CHIRPSv2.0 and ERA5 datasets are selected from the period 1981 – 2022, and all the results described below are based on the ensemble mean of these two datasets.

2.2.2 Normalized Difference Vegetation Index (NDVI) data

NDVI represents the density of greenness over an area by referring to the reflectance in the near-infrared band (NIR) in relationship to the reflectance in the Red band, which is a part of visible shortwave radiation (Rouse et al. in 1974).

The Red band is strongly absorbed by vegetation due to chlorophyll, while vegetation reflects a significant portion of Near-Infrared (NIR) radiation. More NIR radiation is reflected compared to the Red band in dense vegetation, resulting in higher NDVI values. However, in sparse vegetation, the difference between reflected NIR and absorbed Red light is smaller, leading

to lower NDVI values. However, the difference between reflected NIR and absorbed Red light is smaller in sparse vegetation, leading to lower NDVI values. NDVI is defined as:

$$NDVI = \frac{(NIR-Red)}{(NIR+Red)} \quad (1)$$

Theoretically, NDVI ranges from -1.0 to 1.0, although the realistic range is from 0.1 to 1.0 because, in the absence of vegetation, NDVI is close to zero (Alex de la Iglesia Martinez and Labib, 2023). Slightly negative NDVI values have been shown to depict differences in albedo (Alex de la Iglesia Martinez and Labib, 2023); however, these are mostly ignored. In this present study, the NDVI is derived from Terra Moderate Resolution Imaging Spectroradiometer (MODIS) and represented by Vegetation Indices Monthly MOD13C2 Version 6.1, with a spatial resolution of 0.05°. It covers the period 2000–present day. More information about the data can be found in Didan (2021). The data are freely available at https://lpdaac.usgs.gov/products/mod13c2v061/. The NDVI time series with monthly timestep were retrieved from EARTH DATA website by using AppEEARS tool (https://appeears.earthdatacloud.nasa.gov/).

2.3 Methods

2.3.1 Computation of the Standardized Precipitation Index (SPI)

The SPI is used to assess the duration, frequency, severity, and intensity of drought and to identify anomalously dry periods. It is calculated as a standardized departure of observed precipitation from a theoretical probability distribution of the precipitation and can be calculated for different time scales. 2-parameter gamma distribution fit for the SPI calculations (The NCAR Command Language, 2019) was applied in the present study. The gamma distribution parameters were estimated by the maximum likelihood method as described in Thom (1958). The distribution was assessed grid pointwise.

In the present study, we focus on the time scales of three (SPI-3), six (SPI-6), and twelve (SPI-12) months. Following McKee et al. (1993), the SPI is calculated as the difference of the observed precipitation from mean value divided by the standard deviation. Therefore, the value of SPI gives estimate by how many standard deviations the actual precipitation deviates from the theoretical mean value. For SPI-3, -6, and -12, running precipitation averages over 3, 6, and 12 months are assessed, respectively. Previous studies define that the SPI-3 and SPI-6 are normally used to assess agricultural and hydrological droughts, respectively, while the SPI-12 is important in studying groundwater droughts (Elkollaly et al., 2018; Nkunzimana et al., 2021). The classification of wet and dry conditions based on the SPI values is shown in Table 1.

Table 1 Categories of dry and wet conditions based on SPI values following McKee et al. (1993)

SPI value	Category
≥ 2.00	Extremely wet

1.50 to 1.99	Severely wet
1.00 to 1.49	Moderately wet
- 0.99 to 0.99	Near normal
- 1.49 to - 1.00	Moderately dry
- 1.99 to - 1.50	Severely dry
≤ -2.00	Extremely dry

2.3.2 Computation of the SPI on the seasonal and annual scale

To evaluate the drought on a seasonal scale, SPI-6 of April of each year is used to represent the wet season (November-April) and SPI-6 of October for the dry season (May-October). This method was previously used by Elkollaly et al. (2018). Similarly, the same concept was applied for the annual scale by selecting the SPI-12 of December. In further text, we use the terms "seasonal SPI" and "annual SPI".

2.3.3 Drought characteristics - duration, frequency, severity, and intensity

The drought characteristics are calculated as follows:

- Drought duration means the number of months with SPI less than -1 (denoted as $SPI_{\leq -1}$) divided by the number of the events, i.e., the continuous occurrences of the SPI values less than -1:

$$Drought\ duration = \frac{Number\ of\ months\ with\ SPI_{\leq -1}}{Number\ of\ events} \quad (2)$$

- Drought frequency is the percentage of the occurrence of the SPI values less than -1 throughout the study period

$$Drought\ frequency = \frac{Number\ of\ months\ with\ SPI_{\leq -1}}{Number_{Timesteps}} \times 100 \quad (3)$$

Where $Number_{Timesteps}$ is 504 months (the number of months in the study period).

- Drought severity refers to the sum of the SPI values less than -1 over all timesteps:

$$Drought\ severity\ = |\sum SPI_{\leq -1}| \quad (4)$$

- Drought intensity refers to the average of the SPI values less than -1:

$$Drought\ intensity = \frac{Drought\ severity}{Number\ of\ months\ with\ SPI_{\leq -1}} \quad (5)$$

These drought characteristics are calculated for the three considered timescales (SPI3, SPI6, SPI12), and for the seasonal and annual. These written equations are based on the SPI-3, -6 and -12 timescales, however for case of seasonal and annual scales, number of months with SPI less than -1 (SPI≤-1) is replaced by numbers of seasons or years with SP less than -1. Also, the number of timesteps 504 months is replaced by 42 timesteps for seasonal and annual scales.

2.3.4 Computation of correlation

In this study, Pearson and Spearman correlation coefficients were used to quantitatively assess the statistical relationship between SPIs and NDVI anomaly. The Pearson correlation measures the strength of the linear relationship between two variables (Wilks, 2006). Meanwhile, the Spearman correlation assesses the strength and direction of monotonic association between two variables. In other words, it is a calculation of Pearson correlation based on the ranked values of the data (Wilks, 2006). For the calculation of the correlation coefficients, NDVI time series were linearly detrended and its mean seasonal cycle was removed.

3. Results

3.1 Temporal Evolution of SPI

3.1.1 Regional values of monthly SPI-3, SPI-6 and SPI-12

All the three SPI indices shown in Fig. 2-4 exhibit large interannual variability. Dry and wet periods were identified persisting for several years, but also short episodes spanning only a couple of months. Regarding comparison of the three studied regions of Madagascar, between 1981-1986 the SPI evolution for all three timescales was in accord over all three regions. Since then, some event also occurred simultaneously over all three regions (for example the events highlighted by shading, see Section 3.4), but many dry or wet episodes exhibit rather disaccord between the regions. The occurrence of moderate (i.e. SPI values between -1 and -1.49) to severe drought events (i.e. SPI values between -1.5 and -1.99) in the recent decade are more frequent over the southern region (R1) than over the western (R2) and eastern (R3) regions. However, between the years 1995-2005, the drought persisted more over R2 and R3, while R1 experienced rather wetter conditions. The occurrence of extreme drought events (SPI values less than -2) is recorded scarcely in all regions. For SPI-3 and SPI-6, extremely dry years were experienced during 1983, 1992, 2021 and 2022 over the R1, during 1991 and 2017 over the R2, and during 1997 and 017 over the R3. Based on SPI-12 all the regions experienced simultaneous drought in the years 1991, 2006, 2017, and 2021.

3.1.2 Regional values of seasonal and annual SPI

Regarding the SPI for the wet season (SPI-6 for April, Fig. 5A), the results are very similar in R2 and R3 regions, where moderate drought events are recorded during 1988, 1999, 2000, 2006, and 2017. In the southern region R1, the years 1983 and 1992 experienced severe drought events followed by a continuous wetter period until the occurrence of moderate drought in 2010. By the end of the study period, between 2016 and 2022, this region went through consecutive drought, unlike the other

two regions. The temporal development of dry season SPI (Fig. 5B) reveals almost the same pattern in all three regions till 2007. The main features are the occurrence of moderately to extremely wet years at the beginning of the study period from 1981 to 1986, followed by more often dry periods with rather lower magnitude of SPI (the values mostly between –0.5 and –1). The wet events are less frequent after 1986 in the dry season, but the magnitude of SPI is often higher than 1 (Fig. 5B). After 2007, the regions exhibit some dissimilarities from each other, with more occurrences of dry periods over the western and southern regions (R2 and R1). The annual SPI (Fig. 5C) shows different years of moderate to extreme drought events over the three regions, with higher resemblance between R2 and R3. For example, as already seen in Fig. 4, between 1995-2005 the R1 region experienced a relatively wetter period, while in the other two regions the years 1998-2000 were dry with a high magnitude of SPI. It is also worth mentioning that region R1 went through the most severe drought event in the year 2020, while the other two regions had a more severe drought before the year 2000.

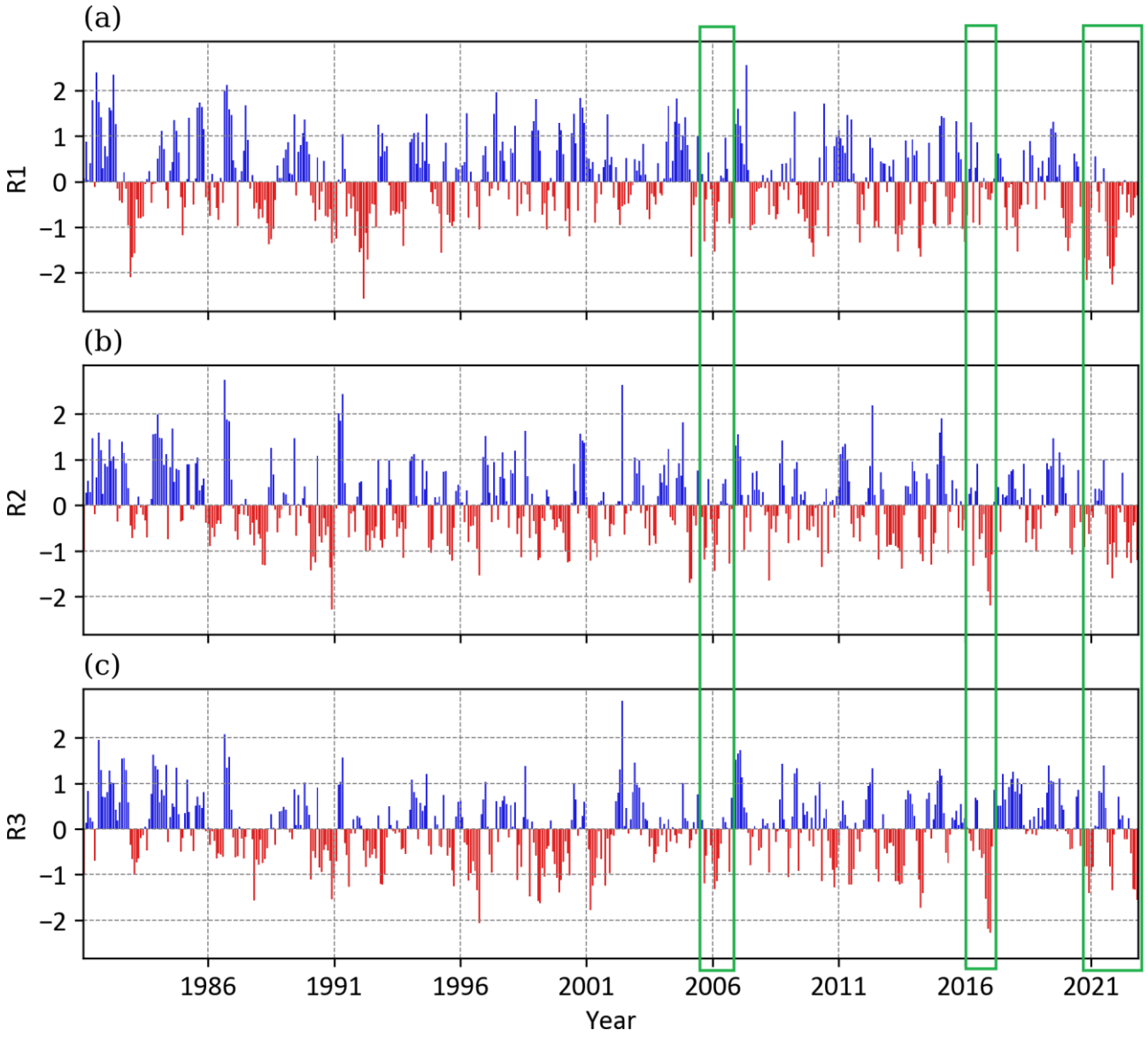

Figure 2: SPI-3 values from the ensemble mean of CHIRPS and ERA5 over Madagascar during the period 1981–2022 over different regions of Madagascar. R1: South, R2: West and R3: East. The green rectangles represent selected periods which will be used for analysis of connection between drought and vegetation.

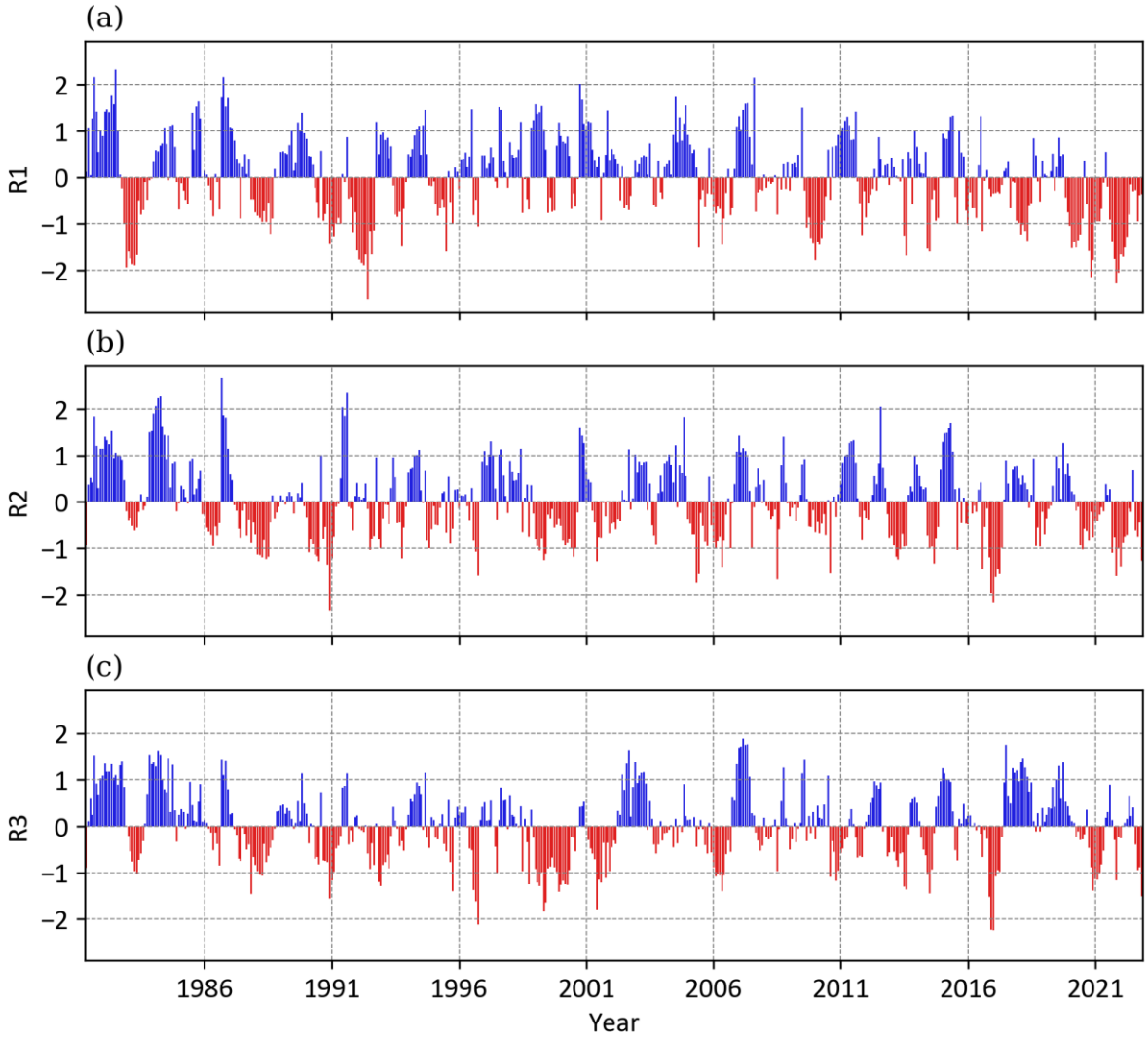

Figure 3: Same as Figure 2 but for SPI-6

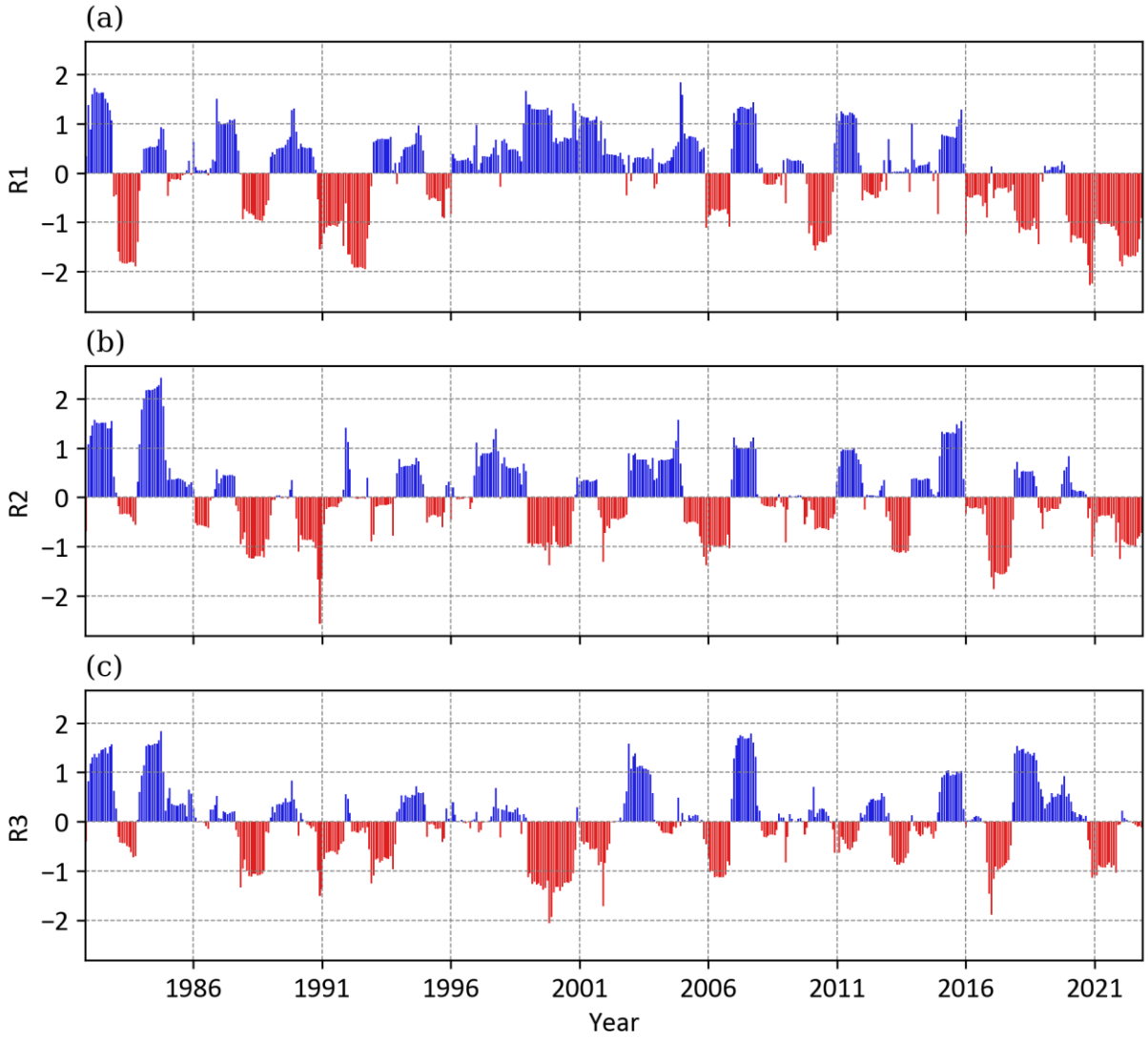

Figure 4: Same as Figure 2 but for SPI-12

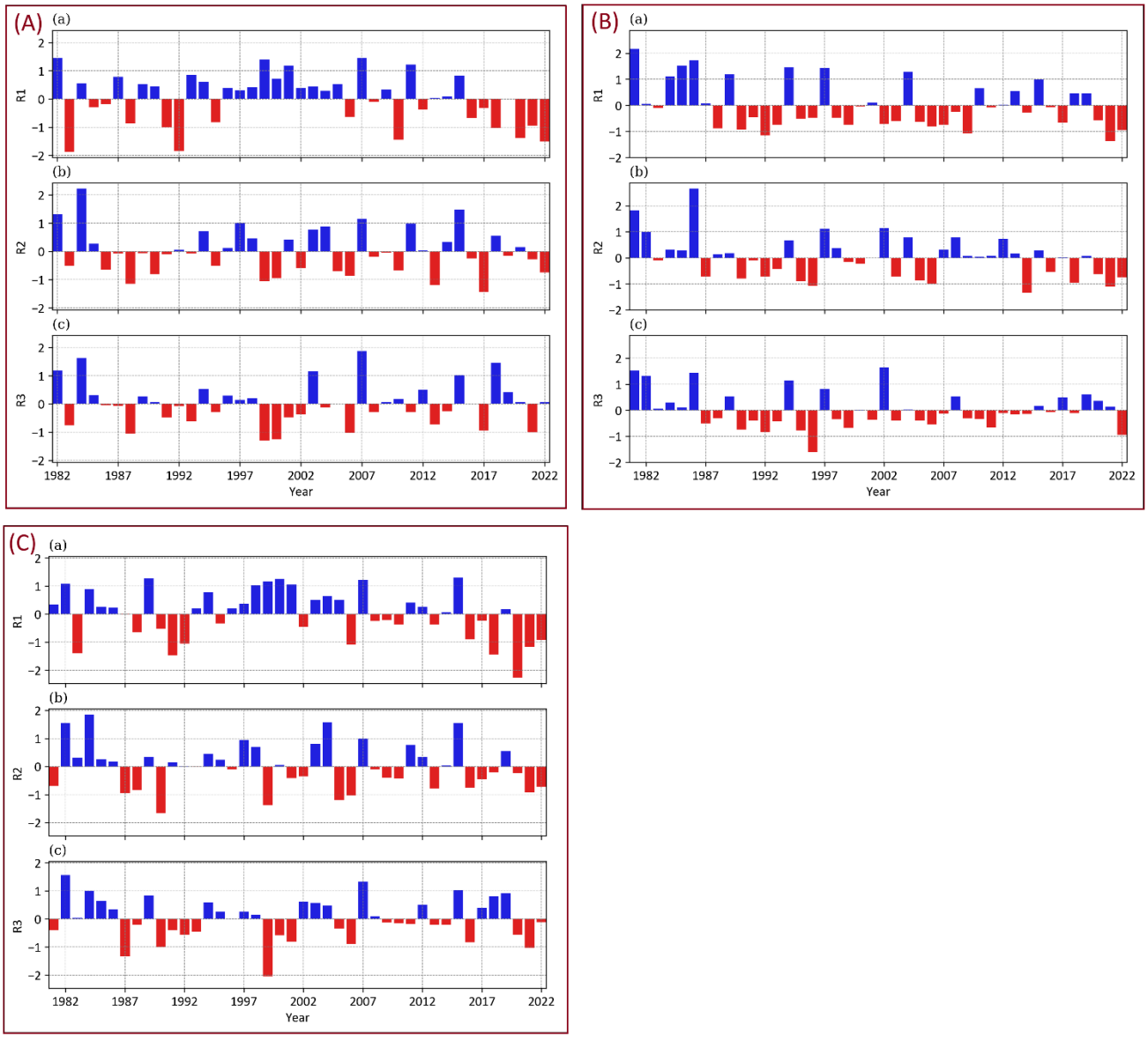

Figure 5: Same as Figure 2, but for (A) seasonal SPI representing the wet season (NDJFMA), (B) seasonal SPI representing the dry season (MJJASO), and (C) annual SPI.

3.2 Spatial analysis of drought characteristics (Duration, Frequency, Intensity, and Severity)

Figure 6 presents the spatial patterns of drought duration, frequency, intensity, and severity for SPI-3, SPI-6, SPI-12 (Fig.6A), and seasonal and annual (Fig.6B) scales. The longest drought duration is observed for SPI-12 (up to more than 10 months in the southern R1 region, Fig. 6Ac), while the shortest drought events are recorded for SPI-3 (less than 2 months, Fig. 6Aa). As explained in McKee et al. (1993), this can be expected concerning the fact that the shorter time scale, the higher variability in

SPI values, resulting in shorter periods of consecutive negative/positive values. But also, higher drought frequency is detected over southern Madagascar for the longer timescale of SPI-12 (22%) compared to SPI-3 (between 10 and 17%, Fig. 6Af and 6Ad, respectively). While SPI-6 displays the same frequency range as SPI-3 but, the areas with higher frequencies have extended. For the case of drought severity, it also increases with increasing time scale, from the least severe over western parts with values of about 75 for SPI-3 to the most severe over the southern parts with values of more than 155 for SPI-12 (Fig. 6Ag, 6Ai). Less severe drought records are found over the western and some of the central parts of the country for all the three SPI indices. Spatial patterns of drought intensity show homogeneous distribution for all three timescales (3, 6, and 12 months, Fig. 6Aj, 6Ak, 6Al) ranging from 1.1 to 2, but the records are gradually increasing from SPI-3 to SP12. The distribution displays higher values over the southern and northern regions, while the central western areas witness lower values. It is worth mentioning that overall, for all three timescales (Fig.6A), the drought characteristics' magnitudes are higher over the eastern and southern regions, especially with prominent values for SPI-12 over the southern part, while some of the western and the central parts display lower values.

Regarding the seasonal values (Fig.6B), the wet season NDJFMA (Fig. 6Ba) displays drought duration values from 0.375 over the southwestern coast to 2.375 [seasons] over the northern parts. On the other hand, the dry season MJJASO (Fig. 6Bc) shows lower drought duration compared to the wet season, with the highest record of 1.875 [seasons] found over the central northern parts. For the annual timescale (Fig.6Bc), drought duration is less than a year over most parts of the country, except over the extreme southern and northern parts, in which the records range between 1.125 and 1.125 [years]. Interestingly, drought duration during wet season and annual scales last longer over some parts of the northern area. Drought occurrence is more frequent during the wet season (Fig. 6Bd, frequency up to 23%), specifically over southern Madagascar, than during the dry season (Fig. 6Be). The seasonal frequency has the same range of values between 5% and 24% for the two seasons, however, larger areas experience more frequent occurrences of drought during the wet season than during the dry season. The annual frequency (Fig. 6Bf) shows drought frequency between 11% and 18% of the study period over most parts of the country. However, some of the northwestern and southern parts witness a frequency up to 23%. The drought severity is larger during the wet season (with values up to more than 14, especially over southern Madagascar, Fig.6Bg) than during the dry season (with maximum severity of up to 11, Fig.6Bh), which is partly due to the frequent occurrence of drought during the wet season (Fig. 6Bd,e). The annual severity reveals that the southern parts of the country record the most severe annual drought of values more than 14 compared to the rest of the areas (Fig.6B1). Regarding the drought intensity, most parts of the country exhibit values between 1.4 and 1.9, except over the central west region with lower values of 1.3 during the wet season (Fig.6Bj). Meanwhile, moderate drought (i.e. $-1.0 \geq SPI \geq -1.49$) dominates during the dry season (Fig. 6Bk) with values between 1.1 and 1.5. In the case of the annual intensity, severe drought ($-1.5 \geq SPI \geq -1.99$ or intensity values between 1.5 and 2) is observed over almost the whole country except the central-west part (Fig. 6Bl) where the intensity is less than 1.5. Overall, based on the seasonal and annual scales analyses, the southern part of Madagascar witnesses higher magnitudes of drought characteristics compared to the rest of the regions, accompanied by an exception of longer drought duration over some parts of the northern areas.

3.3 Potential causes of regional differences in drought characteristics and evolution

Overall, the findings show that the whole country of Madagascar had witnessed drought throughout the past years' records (1891-2022). However, the duration, frequency, severity, and intensity of drought vary from one area to another. The analysis exhibits that the southern part of the country (R1) is more severely affected by drought events than the rest of the country, mainly for SPI-12 (Fig. 2, 3, 4, 5, 6). This region R1 is characterized by a semi-arid climate with annual rainfall of less than 800 mm/year and high annual mean air temperatures ranging between 23°C to 27 °C (Randriatsara et al., 2022a). Regarding potential causes of the above-described drought features, Huang et al. (2017) stated that global warming was observed over the dry land, and the interdecadal variability in aridity changes are regulated by Ocean oscillations which alter the changes in air temperature and rainfall. The impact of rainfall failure in 2019 to 2021 resulted in a severe food security crisis over southern Madagascar, compounded by the already straining impacts of COVID-19 and pest infestation (Harrington et al., 2022). According to Harrington et al. (2022), based on a combination of observations and climate modeling, the increase of poor rains experienced over the southern part of Madagascar was not significantly linked to the anthropogenic climate change because of the overwhelming of the natural variability. However, if the anthropogenic activities increase the global mean temperatures by more than 2 °C above preindustrial levels, the changes in drought will amplify (IPCC 2021; Harrington et al., 2022). This confirms that even though the anthropogenic activities have not been significantly identified as the main cause of changes in drought due to the domination of natural variability, the increase of such activities will expose clearly the amplification of drought events. Other studies on the underlying processes responsible for the strong impact of drought duration and frequency over the southern parts of Madagascar reported an influence of ENSO (El Niño–Southern Oscillation), IOD (Indian Ocean Dipole), and SIOD (sub-tropical IOD) (Hoell et al., 2015; Hart et al., 2018; Barimalala et al., 2018; Randriatsara et al., 2022a). To illustrate, Randriatsara et al. (2022a) remarked that the enhanced (decreased) precipitation during wet (dry) years of the wet and dry seasons in Madagascar is mainly linked to a strong moisture convergence (divergence) accompanied by strong easterlies (anticyclonic circulations) over the northwest (southern) Indian Ocean. The recent study of Barimalala et al. (2024) emphasized that the severe drought over southern Madagascar in 2019 - 2021 was linked to the cold SST anomalies which were the most negative anomalies (precisely the negative SIOD mode) in the past four decades during the rainy season of 2019 and 2020. All these mean that both the anthropogenic activities and the natural variability could have contributed to the drought severity increase over the southern part of the Island.

Generally, drought characteristics across different regions of Africa reveal that Madagascar experiences the shortest drought duration for moderate, severe, and extreme drought categories compared to other climatic zones of Africa (Lim Kam Sian et al., 2023). However, the observed changes in drought characteristics during the recent past (1998 – 2017) are stronger over Madagascar than they were in the far past (1928–1957) (Tall et al., 2023). Moreover, this indicates that the drought events have become more severe in recent years compared to earlier years in Madagascar. In support of that, this study reveals that drought occurrences have become more consecutive over the country, specifically from 2017 to 2022, and intensified over the southern part of the country. This finding aligns with the studies of Harrington et al. (2022) and Rigden et a.l (2024), which

emphasized the increases in drought characteristics over southern Madagascar. Overall, the changes in drought events have been noted over different regions of the world (e.g. Sheffield et al., 2012; Cook et al., 2020) and Africa continent, with numerous studies (e.g. Masih et al., 2014; Nooni et al., 2021; Ayugi et al., 2022; Lim Kam Sian et al., 2023) reporting the heterogeneous patterns of severity, intensity, duration of occurrence and frequencies.

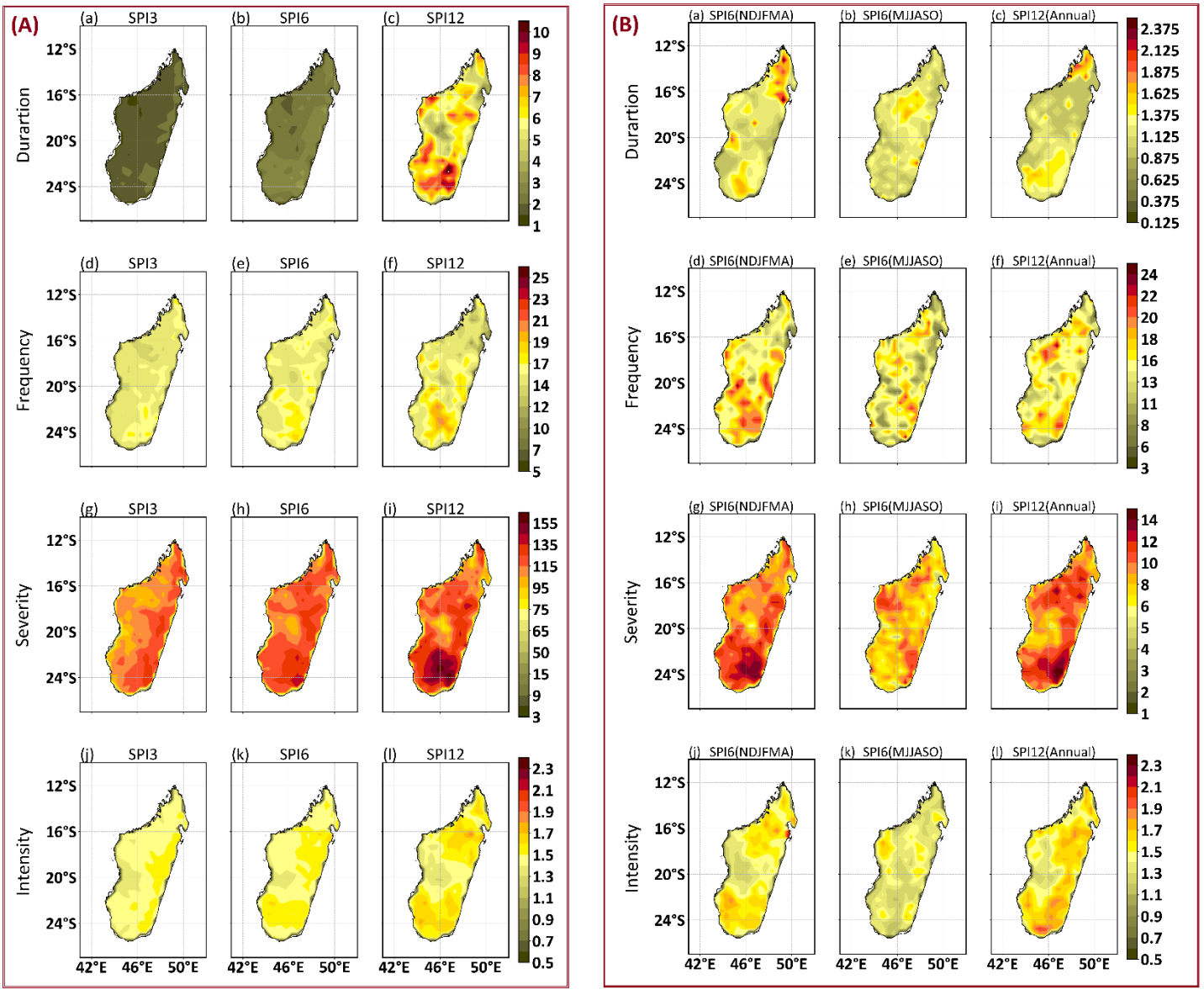

Figure 6: Spatial patterns of drought characteristics described in Section 2.3.3 (A) for SPI-3, -6, and -12 timescales and (B) for seasonal and annual scales. For (A), the units of Duration are [months], of Frequency [%] (the percentage of months with SPI ≤-1 relative to the number of all timesteps), of Severity the sum of SPI ≤-1, and of Intensity it is the average of the severity during the months with SPI ≤-1. For seasonal and annual scales (panel B), the units of the Duration are [seasons] for the case of season and

[years] for the annual scale. Frequency, severity and intensity in (B) have the same units as in (A), only the timesteps are seasons and years instead of months. The figure shows the averaged values of duration, frequency and intensity, but for severity, it represents the accumulation of all values ≤-1.

3.4 Impact of drought on Vegetation

To compare NDVI in different months and locations, differences (anomalies) of individual NDVI values against NDVI mean throughout the study period were calculated.

First, to study the impact of drought on vegetation, the three most severe drought episodes affecting the whole of Madagascar were selected. The selection was based both on the SPI values for each of the regions from Fig. 2-4 (as marked with green rectangles in Fig. 2) and the SPI values averaged over the whole island (Fig. S1). The episodes will be further denoted as "Event-I" (spanning October 2005 - October 2006), "Event-II" (January 2016 - April 2017), and "Event-III" (September 2020 - December 2022).

3.4.1 NDVI differences based on the selected drought episodes

Analyzing the spatial distribution of the NDVI anomalies before and after the three selected drought episodes reveals some contradictory findings. The results agree with intuitive expectations in the case of Event-I: NDVI anomalies at the end of the Event-I (Fig. 7d) show that the areas with negative values (between -0.03 and -0.06) expand to the south and some parts of the north compared to the beginning of the event (Fig. 7a). This means that vegetation cover has decreased after the continuous occurrence of the negative SPI values during the Event-I. Similarly, the Event-II (Fig. 7b, 7e) shows expanded areas affected by negative anomalies between -0.03 and -0.18 by the end of the event (Fig. 7e). Surprisingly, the Event-III (Fig. 7c, 7f) shows contradictory outcomes, with the southern part of the island exhibiting more vegetation losses at the beginning of the event, though enhanced vegetation at its ending. This is well perceived over the southern part of Madagascar, where the negative NDVI anomalies cover almost the south with values between -0.03 and -0.15 at the beginning of Event-III (Fig. 7c), but the values turn significantly to positive up to 0.21 over most part of the Country by the end of the event (Fig. 7f). Though, some parts over the southeast and some tiny spots along the southern coastline remain with negative values up to -0.18 (Fig. 7f).

Therefore, additional analyses were performed to comprehend the increase in vegetation cover during the Event-III (Fig. 7c, 7f). NDVI differences for each month of Event-III against the corresponding month-mean throughout the study period are shown in the additional Fig. S3. The vegetation cover gradually enhances from January 2016 until it reaches the peak of positive NDVI anomalies of about 0.3 in April 2016. Afterward, negative NDVI anomalies intensify gradually from May, reaching their lowest values between September and November 2016. Then, vegetation begins to recover in December until it reaches its positive peak again in April 2017. Several other years were also analyzed (not shown here), and it was confirmed that the annual course is similar like in 2016 and 2017, illustration for 2022 is shown in Fig. S4. This suggests that it is not appropriate to assess vegetation loss based on a single month by referring to the starting and ending months of the continuous

occurrence of negative SPI values. This is because whenever the starting month falls within the negative peak months (from August to November, Fig.S3 and S4) and the ending month falls in other months, the intensity of vegetation loss is always greater during these negative peak months than in other months. Therefore, the comparison of anomalies should be performed between the same month from different years. For instance, more decline in vegetation cover is found in January 2022 (Fig. S4a) compared to January 2016 (Fig. S3a). This is relevant without the influence of seasonal rainfall and can be used to examine the impact of negative SPI values on vegetation changes for a specific month from different years.

Furthermore, the significant vegetation loss over the southern region during January and February (Fig. S4), i.e. in the middle of wet season (from November to April), is apparently related to the changes in seasonal rainfall over Madagascar, specifically the delaying and shortening of the rainy season in recent years over the region (Harrington et al., 2022). It has been found that the delayed and shortened rain during the wet season influences vegetation decline over the southern region (Rigden et al., 2024). This is obvious since the dry season of the country lasts from May to October; however, the onset of the rainy season over the southern region has delayed till December and January due to not only natural variability such as poleward migration of the mid-latitude jet (Rigden et al., 2024) but also the anthropogenic climate change (Dunning et al., 2018; Rigden et al., 2024). Therefore, it is unsurprising that the southern region experiences vegetation losses even in January and February, while the vegetation over the northern and eastern regions has started to grow already.

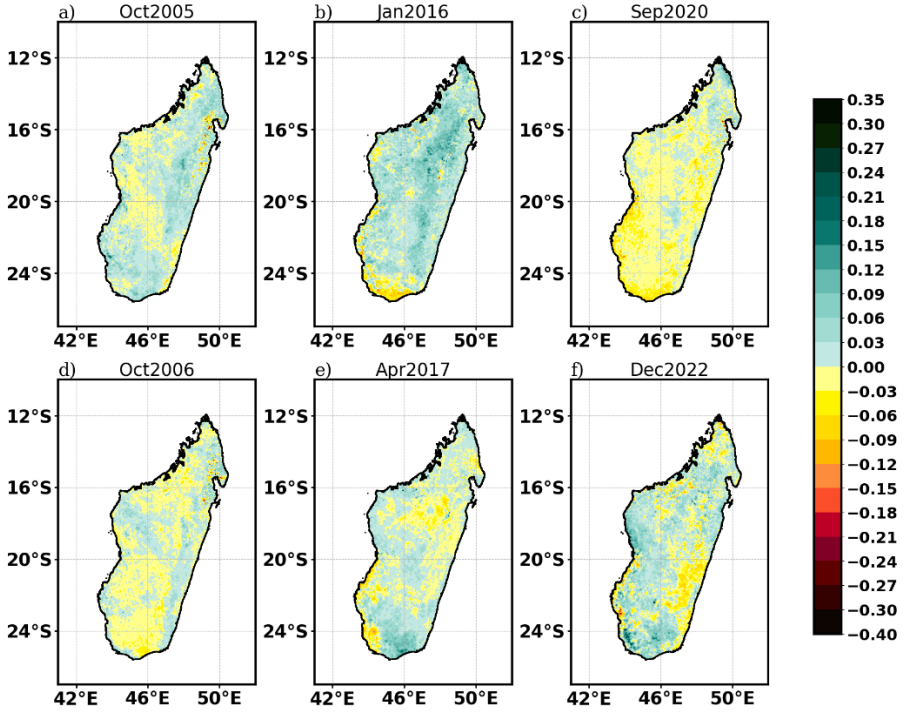

Figure 7: NDVI difference between selected month and the corresponding monthly mean over the study period 2000-2022. The selected months represent the start and end of the events with continuous occurrence of negative values of the SPI-3, SPI-6 and SPI-12 as marked with green rectangles in Fig. S1 and S2. Panels a) and d) represent the beginning and the ending of the first occurrence

of continuous negative SPI values (Event-I); panels b) and e) represent the second occurrence (Event-II); panels c) and f) represent the third occurrence of continuous negative SPI values (Event-III).

3.4.2 Impact of drought in years selected based on seasonal and annual SPI

In this part, Event-I and Event-III are further analyzed since the continuous negative SPI values on seasonal and annual scales occur only for these two events (Fig. S2). Figure 8 presents NDVI annual mean anomalies of the selected years from Event-I and Event-III against the NDVI year mean throughout the study period. The Event-I starts in 2005 and ends in 2006 by referring to the annual and seasonal SPI in Fig. S2. The decrease in vegetation has intensified during this event. For instance, in 2005 the western part (between 16°S and 20°S) and some of the central part of the country displayed negative NDVI anomalies of about -0.03, while the rest of the areas recorded positive values between 0.03 and 0.21 (Fig. 8a). By 2006, which was the end of Event-I, the decrease in vegetation extended to larger areas over the southern region and some parts of the north with an increased NDVI anomalies of up to -0.06 (Fig. 8c). Similar patterns are found during Event-III occurring from 2020 to 2022 (Fig. 8b). In 2020, the southern region exhibited negative NDVI anomalies between -0.03 and -0.12 with a tiny spot of -0.15 over the south-western part. While the northern part is sparsely mixed with negative and positive anomalies ranging from -0.12 to 0.18. However, by the end of the Event-III in 2022 (Fig. 8d), the areas with negative anomalies expanded with increased values up to -0.18 over the southern region, while negative anomalies dominate the northern region.

These results suggest that the continuous occurrence of negative seasonal and annual SPI values (Fig. S2) enhances and spreads vegetation losses by the end of a drought event. In other words, the findings indicate that continuous negative values of seasonal and annual SPI can be used to examine vegetation changes over Madagascar. This agrees with other studies (Nicholson et al., 1990; Camberlin et al., 2007; Zhang et al., 2023), which demonstrated that the inter-annual variations of the vegetation cover are correlated with annual and seasonal rainfall fluctuations.

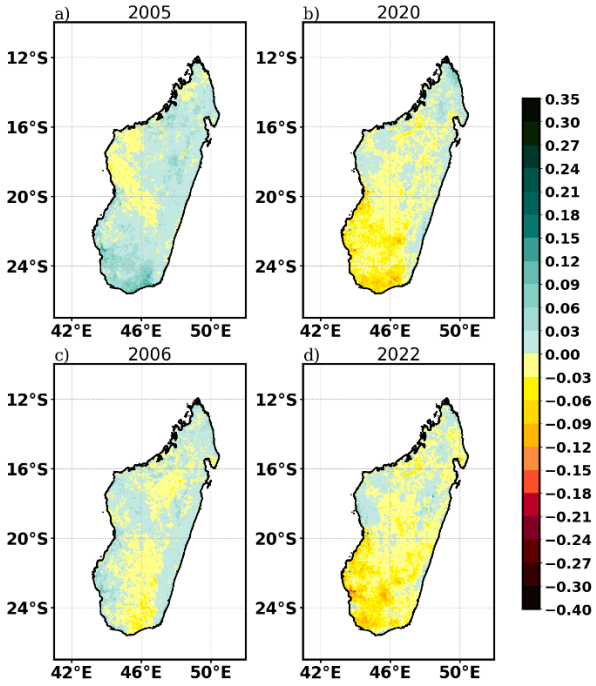

Figure 8: NDVI difference (anomaly) between selected years and the NDVI yearly mean throughout the whole study period. The years are selected based on the continuous negative SPI values found during the seasonal analysis from Fig. S2 as marked with green rectangles. a) and c) represent the difference at the beginning and the ending of the first occurrence of continuous negative SPI values, respectively. b) and d) represent the difference at the beginning and the ending of the second occurrence of continuous negative SPI values, respectively.

3.4.3 Vegetation response to the lowest values of wet season SPI

Another perspective on the impact of drought on vegetation is presented in Fig. 9, which shows seasonal and annual NDVI anomalies for the years 2006, 2017 and 2021, chosen based on the lowest wet season SPI values (Fig. S2a, marked with green circles). The interest is only to analyze the wet season in which the lower SPI values are detected, to see the impact of rainfall scarcity on vegetation. The results show that the smaller negative SPI amplitudes found in these selected years during the wet season (as marked in Fig. S2a) have huge impacts on declining the wet season vegetation amounts (Fig. 9a, 9d, 9g) over the whole study area compared to the dry season (Fig. 9b, 9e and 9h) and the annual scale (Fig. 9c, 9f, 9i). It is also worth mentioning that the intensity of the vegetation loss during the wet season of these selected years has gradually increased from -0.03 to -0.24 of NDVI, especially over the southern part of the country (Fig. 9g). However, vegetation during the dry season (Fig. 9b, 9e, 9h) has improved over most parts of the country with NDVI values up to 0.15, except in some parts of the southern region. Besides, the vegetation changes for each year (Fig. 9c, 9f, 9i) show that more than half of the country experiences vegetation loss in 2017 and 2021 with NDVI anomaly values between -0.03 and -0.18 with higher amplitude values found in the southern part of the country.

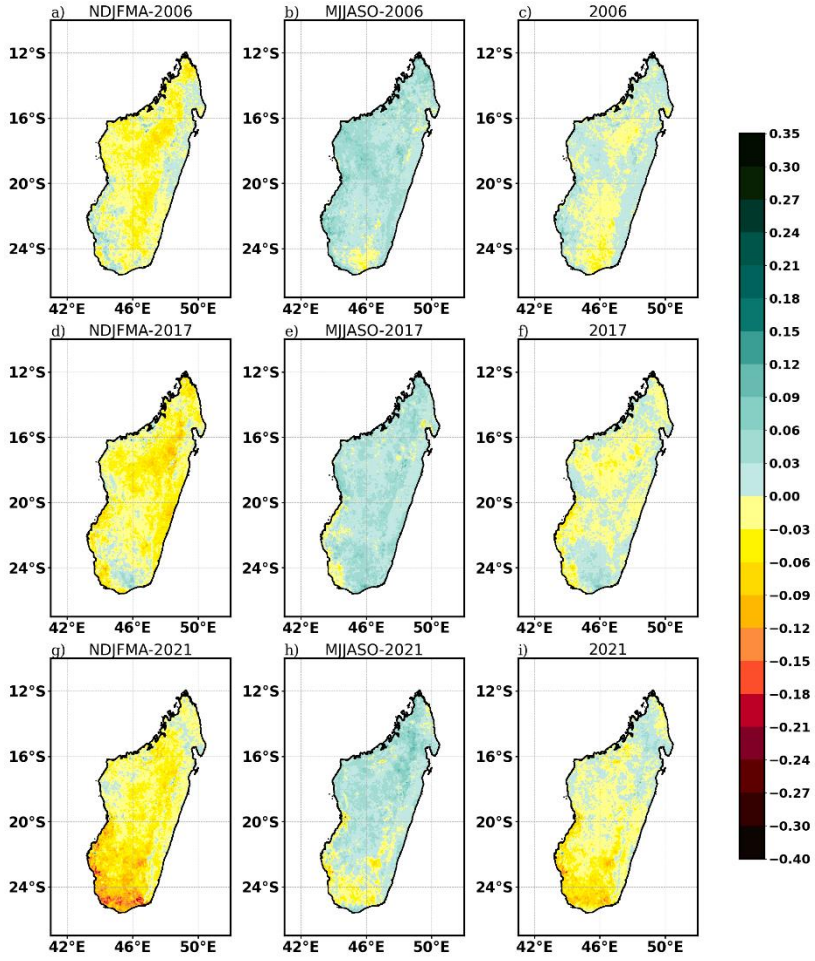

Figure 9: Seasonal and annual NDVI difference between selected years and NDVI seasonal and annual mean throughout the study period. The years 2006, 2017 and 2021 were chosen based on smaller negative values found during the wet season from Fig. S2a as marked with green circles. a), d), g) represent the differences during the wet season of each mentioned year. b), e), h) represent the differences during the dry season of each mentioned year. c), f), i) represent the differences for the annual averaged NDVI of each mentioned year.

The severe vegetation decrease found over southern Madagascar necessitated further analysis of the temporal development of annual mean NDVI in Fig. 10. Obviously, the highest NDVI values are seen for the eastern region (R3), which is the rainy forest region, followed by western region (R2), and the southern region (R1) with the lowest NDVI amounts. This clearly corresponds to the ecoregions and climatic types over Madagascar (Burgess et al., 2004; Desbureaux and Damania, 2018). Regarding the interannual variability, rather stable annual mean values of NDVI ranging from 0.62 to 0.66 (0.46-0.48) are seen over the R3 (R2) region (Fig. 10). However, a considerable NDVI decline has occurred over the R1 region, with decreasing values from 0.44 to 0.35 by the end of the study period (Fig. 10). The linear trend for R1 is statistically significant

at 95% confidence level with p-value of about 0.00006877. To better detect this interannual NDVI decline over southern Madagascar, temporal development of monthly NDVI values is performed in Fig. S5. It shows that the variability over R2 and R3 is rather low even for the monthly values. However, the R1 region exhibits a noticeable vegetation decrease from November to March (Fig. S5). The peak of the decline is captured in January, in which the NDVI is recorded of about 0.55 in 2000 and reduced to about 0.32 in 2022. This severe decline found in January and February in the most recent years over southern Madagascar has been explained earlier that it could be due to the delayed onset of the wet season rainfall over that region, which is caused by the natural variability (Harrington et al., 2022; Rigden et al., 2024) and the anthropogenic climate change (Dunning et al., 2018; Rigden et al., 2024). Moreover, these latter analyses (Fig. 10 and Fig. S5) show that the vegetation decline over the southern region intensifies along with the most recent years (2019-2022). It has already been noticed from SPI analysis (Fig.2-5) that the occurrence of drought has recently become more frequent and intense, specifically over the southern region, during the most recent years. This could be among the reasons for the severe vegetation decline over the southern region in the most recent years of the study period (see also 3.1).

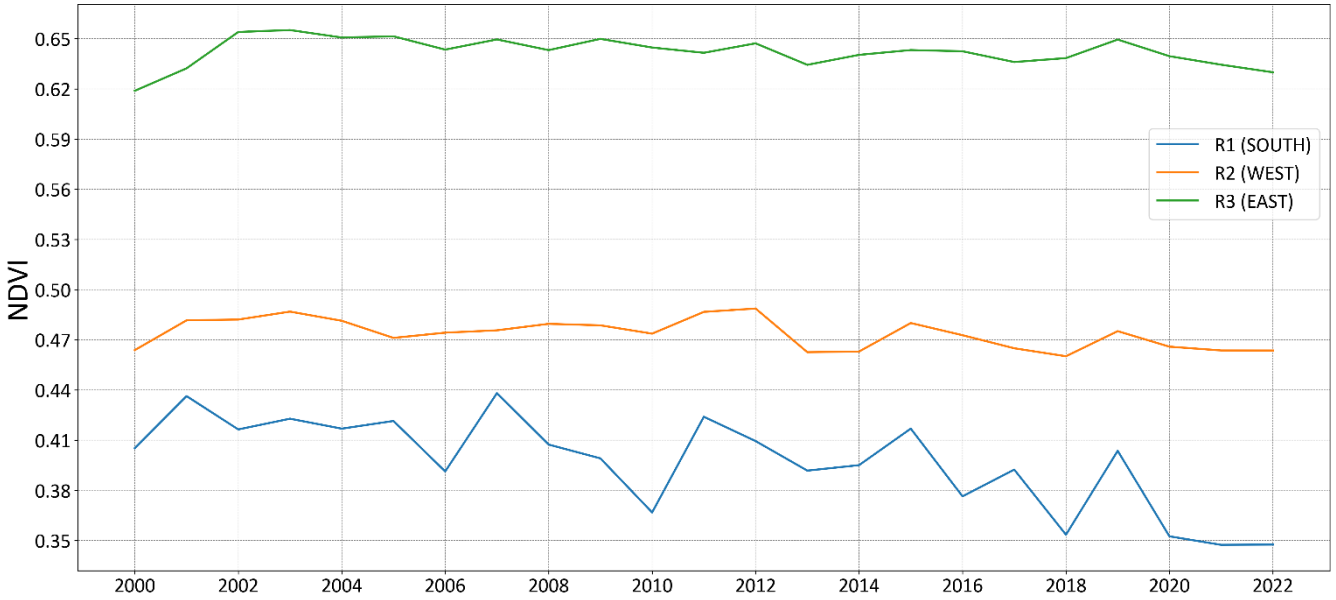

Figure 10: Interannual variability of NDVI over different regions of Madagascar: R1: South, R2: West and R3: East.

3.3.4 Correlation between SPI and NDVI

To assess the NDVI-SPI relationship in a quantitative way, we calculated correlations between the two variables over the period 2000-2022 (see Section 2.3.4). Temporal correlation analyses based on Pearson and Spearman coefficients (Fig. S6) were performed between the NDVI anomaly and each SPI timescale (SPI-3, -6, and -12) over each region. The results show a

positive correlation over all the regions. However, it is worth mentioning that the southern region (R1) exhibits higher correlation coefficient values of about 0.12 to 0.21 compared to the regions R2 and R3 (between 0.04 and 0.19). This suggests that, even though low correlation coefficients are found, there is a connection between vegetation changes and the occurrence of drought events, while the connection is more emphasized over the southern region (R1) than over the two other regions. To better identify the connection, spatial distributions of Pearson correlation between NDVI anomaly and each SPI are performed in Fig. 11. For the case of SPI-3 and SPI-6 (Fig. 11a, 11b), more than half of the country exhibits a statistically significant correlation at 95% confidence level with values of correlation between 0.1 and 0.5. But for the SPI-12, the correlation is only significant over the southern and some parts of the northern region (Fig. 11c). This suggests that drought occurrences impact vegetation's cover, especially over the southern region. It is worth mentioning that, even though the correlation coefficient values are generally low (i.e. less than 0.5), they are statistically significant at the 95% confidence level. This indicates that drought occurrences are indeed among the factors contributing to the deterioration of Madagascar's vegetation. However, it is not only drought that caused the changes in vegetation, but there are also other factors, such as human-induced deforestation as the population relies heavily on fuelwood. Moreover, the drought also leads to deforestation as farmers clear local forests to adverse effects of drought on agricultural productivity (Desbureaux and Damania, 2018). The latter could be among the reasons that amplifies higher positive correlation coefficients found between vegetation index and drought index over southern Madagascar (Fig. 11) due to the occurrence of more frequent and intense drought over that region. Moreover, Duku et al. (2021) reported that the significant human induced deforestation over local and non-local areas is among the factors that lead to a shortening of the wet season rainfall over southern Madagascar. This is obvious since deforestation has an indirect effect on trends in water availability by interacting with the atmosphere, as warming and drying tend to be caused by deforestation, resulting in precipitation decreases (Butt et al., 2011; Wright et al., 2017). Additionally, according to the reviews by Staten et al. (2020) and Xian et al., (2021), the expansion of Hadley cell in response to anthropogenic climate change leads to the drying condition of southern Madagascar. All of these factors which trigger precipitation reductions worsen vegetation losses over the southern region compared to other regions of the country. On the other hand, the vegetation over western Madagascar shows weaker correlation with drought index for all the three SPI timescales. This could be due to the vegetation characteristic over the region, which is a dry forest able to survive even under dry conditions (Desbureaux and Damania, 2018; Lawal et al., 2021).

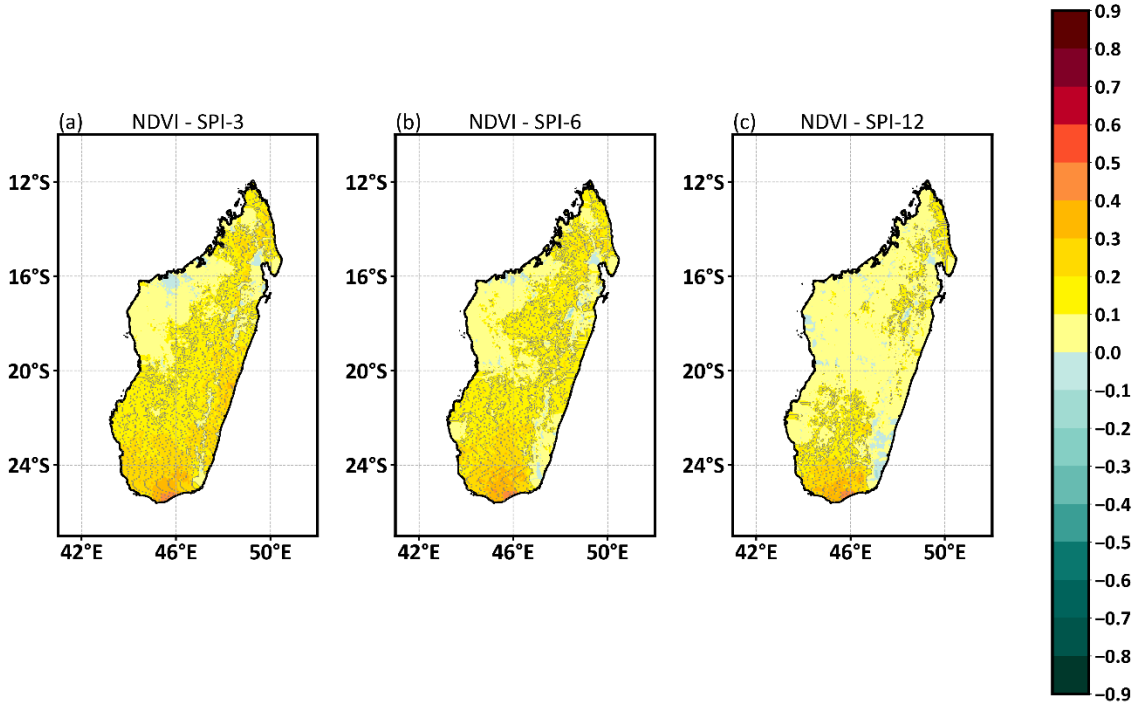

Figure 11: Spatial distribution of the Pearson correlation between detrended NDVI anomaly and drought index for all three timescales (SPI-3, -6, -12). Dotted areas are statistically significant at 95% confidence level using a student's t-test.

4. Conclusion

In summary, the aim of this study was twofold. Firstly, we analyzed the temporal development of SPI over Madagascar during 1981-2022 and the spatial distribution of the drought characteristics (duration, frequency, severity, intensity). Secondly, we assessed the relationship between SPI and NDVI during 2000-2022, representing the impact of drought on vegetation over the studied area.

i) This study reveals that drought occurrences have become more consecutive over the country, specifically during the most recent past (2017 to 2022), and intensified over the southern part of the country. This finding aligns with what has been found by Harrington et al. (2022), Tall et al. (2023), Rigden et al. (2024), and Barimalala et al. (2024).

ii) The study also confirms that the occurrence of continuous negative values of seasonal and annual SPI (Fig. S2) can be used to examine vegetation changes over Madagascar. The result shows that vegetation losses have increased at the end of such occurrence. For instance, the years 2006 and 2022 (Fig. S2) are the ends of the continuous occurrences of drought events, during which the decreases in vegetation cover are detected,

especially over the southern part of the country (Fig. 8). Similarly, smaller negative values of the wet season SPI (Fig. S2a) can be employed to inspect vegetation losses during that season. The finding reveals that these smaller SPI values have a huge impact on vegetation degradation of Madagascar during the wet season. For instance, the years 2006, 2017 and 2021 (Fig. S2a) represent smaller negative SPI values during the wet seasons, which display more vegetation losses over almost the whole country in these wet seasons compared to the dry seasons and the annual analyses (Fig. 9).

iii) The relationship (quantified by the correlation) between vegetation and drought index is strongest over the southern, whereas in the western part the correlation is lower. Among other reasons, we hypothesize that this could be due to different vegetation types. Dry forest over the western part of Madagascar is less vulnerable to drought than those of the southern and eastern. Moreover, the link found between more severe drought and vegetation losses over southern Madagascar (R1) compared to the western (R2) and eastern (R3) regions could happen due to diverse factors that contribute to rainfall deficit over that region. These factors delay and shorten seasonal rainfall and are caused by both natural variability (Harrington et al., 2022; Rigden et al., 2024) and anthropogenic climate changes (Dunning et al., 2018; Rigden et al., 2024).

There are potentially other climatic factors influencing vegetation besides drought, e.g., changes in air temperature distribution and humidity, possibly connected to some large-scale circulation changes. Further, there are probably non-climatic anthropogenic factors, mainly deforestation and agricultural activities in the area. However, the analysis of these factors is beyond the scope of the present study and would be considered for the next research.

Code availability. Drought characteristics computation codes are available on request from the main author, Herijaona Hani-Roge Hundilida Randriatsara. The SPI calculation is available on the NCL website (https://www.ncl.ucar.edu/Applications/spi.shtml, NCAR Command Language).

Data availability. The ERA5 dataset is available on the Copernicus Climate Change Service (C3S) website at https://cds.climate.copernicus.eu/cdsapp#!/home. The CHIRPS v2.0 data is available at https://iridl.ldeo.columbia.edu/SOURCES/.UCSB/.CHIRPS/.v2p0/.daily-improved/.global/.0p05/.prcp. The NDVI time series with monthly timestep were retrieved from EARTH DATA website by using AppEEARS tool (https://appeears.earthdatacloud.nasa.gov/) and are freely available at https://lpdaac.usgs.gov/products/mod13c2v006/. The outputs data sets can be accessed through the reference Randriatsara et al. (2024).

Author contributions. Herijaona Hani-Roge Hundilinda Randriatsara: Conceptualization, data curation, formal analysis, methodology, original draft writing. Eva Holtanova: Conceptualization, Project administration, review and editing, supervision, funding acquisition, validation. Karim Rizwan: Data analysis, software and scripts. Hassen Babaousmail: Data analysis, software and scripts. Mirindra Finaritra Rabezanahary Tanteliniaina: Software and scripts. Kokou Romaric Posset:

Writing, review and editing. Donnata Alupot: Writing, review and editing. Brian Ayugi: Conceptualization, original draft writing, review and editing.

Conflict of Interest. No convection-permitting conflict of interest amongst the authors.

Acknowledgment. The authors are grateful to the Johannes Amos Comenius Programme (P JAC) which supports this research, as well as to the data centers for availing the datasets that were so instrumental in accomplishing the task.

Funding. This research was supported by the Johannes Amos Comenius Programme (P JAC) project No. CZ.02.01.01/00/22_008/0004605, Natural and anthropogenic georisks.

References

Alex de la Iglesia Martinez, S. M. Labib: Demystifying normalized difference vegetation index (NDVI) for greenness exposure assessments and policy interventions in urban greening, Environ. Res., 220, 115155, https://doi.org/10.1016/j.envres.2022.115155, 2023.

Ayugi, B. O., Eresanya, E. O., Onyango, A. O., Ogou, F. K., Okoro, E. C., Okoye, C. O., Okenwa, E. O., Siyanbola, W. A., Maduako, R. E., and Akintoye, S. A.: Review of meteorological drought in Africa: historical trends, impacts, mitigation measures, and prospects, Pure Appl. Geophys., 179, 1365-1386, https://doi.org/10.1007/s00024-022-02988-z, 2022.

Barimalala, R., Desbiolles, F., Blamey, R. C., and Reason, C.: Madagascar influence on the South Indian Ocean convergence zone, the Mozambique Channel trough and Southern African rainfall, Geophys. Res. Lett., 45, 11380-11389, https://doi.org/10.1029/2018GL079964, 2018.

Barimalala, R., Wainwright, C., Kolstad, E. W., Demissie, T. D.: The 2019–21 drought in southern Madagascar, Weather Clim. Extrem., 46, 2212-0947, https://doi.org/10.1016/j.wace.2024.100723, 2024.

Belda, M., Holtanová, E., Halenka, T., and Kalvová, J.: Climate Classification Revisited: From Koppen to Trewartha, Clim. Res., 59, 1-13, https://doi.org/10.3354/cr01204, 2014.

Bennett, A. C., McDowell, N. G., Allen, C. D., and Anderson-Teixeira, K. J.: Larger trees suffer most during drought in forests worldwide, Nat. Plants, 1, 15139, https://doi.org/10.1038/nplants.2015.139, 2015.

Burgess, N., Hales, J., Underwood, E., Dinerstein, E., Olson, D., Itoua, I., Schipper, J., Ricketts, T., and Newman, K.: Terrestrial eco-regions of Africa and Madagascar: A conservation assessment, World Wildlife Fund, ISBN: 1-55963-364-6, https://www.researchgate.net/publication/292588815, 2004.

Butt, N., de Oliveira, P. A., and Costa, M. H.: Evidence that deforestation affects the onset of the rainy season in Rondonia, Brazil, J. Geophys. Res. Atmos., 116, D11120, https://doi.org/10.1029/2010JD015174, 2011.

Camberlin, P., Martiny, N., Philippon, N., and Richard, Y.: Determinants of the interannual relationships between remote-sensed photosynthetic activity and rainfall in tropical Africa, Remote Sens. Environ., 106, 199-216, https://doi.org/10.1016/j.rse.2006.08.009, 2007.

Chaves, M. M., Maroco, J. P., and Pereira, J. S.: Understanding plant responses to drought from genes to the whole plant, Funct. Plant Biol., 30, 239-264, https://doi.org/10.1071/FP02076, 2003.

Cook, B. I., Mankin, J. S., Marvel, K., Williams, A. P., Smerdon, J. E., and Anchukaitis, K. J.: Twenty–first Century Drought Projections in the CMIP6 Forcing Scenarios, Earth's Future, 8, https://doi.org/10.1029/2019EF001461, 2020.

Desbureaux, S., and Damania, R.: Rain, forests and farmers: Evidence of drought-induced deforestation in Madagascar and its consequences for biodiversity conservation, Biol. Conserv., 217, 337-347, https://doi.org/10.1016/j.biocon.2018.03.005, 2018.

Didan, K.: MODIS/Terra Vegetation Indices Monthly L3 Global 0.05 Deg CMG, NASA EOSDIS LP DAAC, https://lpdaac.usgs.gov/products/mod13c2v006/, last access: 10 September 2023.

Duku, C., and Hein, L.: The impact of deforestation on rainfall in Africa: a data-driven assessment, Environ. Res. Lett., 16, 064044, https://doi.org/10.1088/1748-9326/abfcfb, 2021.

Dunning, C. M., Black, E., and Allan, R. P.: Later wet seasons with more intense rainfall over Africa under future climate change, J. Clim., 31, 9719-9738, https://doi.org/10.1175/JCLI-D-18-0102.1, 2018.

Elkollaly, M., Khadr, M., and Zeidan, B.: Drought analysis in the Eastern Nile basin using the standardized precipitation index, Environ. Sci. Pollut. Res., 25, 10265-10278, https://doi.org/10.1007/s11356-016-8347-9, 2018.

Funk, C., Peterson, P., Landsfeld, M., Pedreros, D., Verdin, J., Shukla, S., Husak, G., Rowland, J., Harrison, L., Hoell, L., and Michaelsen, J.: The climate hazards infrared precipitation with stations - A new environmental record for monitoring extremes, Sci. Data, 2, 150066, https://doi.org/10.1038/sdata.2015.66, 2015.

Gouveia, C. M., Trigo, R. M., Beguería, S., and Vicente-Serrano, S. M.: Drought impacts on vegetation activity in the Mediterranean region: An assessment using remote sensing data and multi-scale drought indicators, Glob. Planet. Change, 151, 15-27, https://doi.org/10.1016/j.gloplacha.2016.06.011, 2017.

Harrington, L. J., Wolski, P., Pinto, I., Ramarosandratana, A. M., Barimalala, R., Vautard, R., Philip, S., Kew, S., Singh, R., Heinrich, D., Arrighi, J., Raju, E., Thalheimer, L., Razanakoto, T., Aalst, M., Li, S., Bonnet, R., Yang, W., Otto, F., and Oldenborgh, G.: Limited role of climate change in extreme low rainfall associated with southern Madagascar food insecurity, 2019–21, Environ. Res. Clim., 1, 021003, https://doi.org/10.1088/2752-5295/aca695, 2022.

Hart, N. C., Washington, R., and Reason, C. J. C.: On the likelihood of tropical–extratropical cloud bands in the South Indian convergence zone during ENSO events, J. Clim., 31, 2797-2817, https://doi.org/10.1175/JCLI-D-17-0221.1, 2018.

Heim, R. R. Jr.: A review of twentieth-century drought indices used in the United States, Bull. Am. Meteorol. Soc., 83, 1149-1166, https://doi.org/10.1175/1520-0477-83.8.1149, 2002.

Hersbach, H., Bell, B., Berrisford, P., Hirahara, S., Horányi, A., Muñoz-Sabater, J., Nicolas, J., Peubey, C., Radu, R., Schepers, D., Simmons, A., Soci, C., Abdalla, S., Abellan, X., Balsamo, G., Bechtold, P., Biavati, G., Bidlot, J., Bonavita, M., Chiara, G. D., Dahlgren, P., Dee, D., Diamantakis, M., Dragani, R., Flemming, J., Forbes, R., Fuentes, M., Geer, A., Haimberger, L.,

Healy, S., Hogan, R. J., Hólm, E., Janisková, M., Keeley, S., Laloyaux, P., Lopez, P., Lupu, C., Radnoti, G., De Rosnay, P., Rozum, I., Vamborg, F., Villaume, S., and Thépaut, J.: The ERA5 global reanalysis, Q. J. R. Meteorol. Soc., 146, 1999–2049, https://doi.org/10.1002/qj.3803, 2020.

Hoell, A., Funk, C., Magadzire, T., Zinke, J., and Husak, G.: El Nino–Southern Oscillation diversity and Southern Africa teleconnections during Austral Summer, Clim. Dyn., 45, 1583–1599, https://doi.org/10.1007/s00382-014-2414-z, 2015.

Huang, J., Li, Y., Fu, C., Chen, F., Fu, Q., Dai, A., Shinoda, M., Ma, Z., Guo, W., Li, Z., Zhang, L., Liu, Y., Yu, H., He, Y., Xie, Y., Guan, X., Ji, M., Lin, L., Wang, S., Yan, H., and Wang, G.: Dryland climate change: Recent progress and challenges, Rev. Geophys., 55, 719–778, https://doi.org/10.1002/2016RG000550, 2017.

Huang, S., Tang, L., Hupy, J. P., Wang, Y., and Shao, G.: A commentary review on the use of normalized difference vegetation index (NDVI) in the era of popular remote sensing, J. For. Res., 32, 1–6, https://doi.org/10.1007/s11676-020-01155-1, 2021.

Huete, A., Didan, K., Miura, T., Rodriguez, E. P., Gao, X., and Ferreira, L. G.: Overview of the radiometric and biophysical performance of the MODIS vegetation indices, Remote Sens. Environ., 83, 195–213, https://doi.org/10.1016/S0034-4257(02)00096-2, 2002.

IPCC: Summary for policymakers, in: Climate Change 2021 – The physical science basis: Working Group I contribution to the sixth assessment report of the Intergovernmental Panel on Climate Change, Cambridge University Press, 3–32, https://doi.org/10.1017/9781009157896.001, 2021.

Jury, M., Parker, B. A., Raholijao, N., and Nassor, A.: Variability of summer rainfall over Madagascar: Climatic determinants at interannual scales, Mon. Weather Rev., 15, 1323–1332, https://doi.org/10.1175/MWR-D-15-0077.1, 1995.

Kalisa, W., Zhang, J., Igbawua, T., Ujoh, F., Ebohon, O. J., and Namugiza, J.: Spatio-temporal analysis of drought and return periods over the East African region using Standardized Precipitation Index from 1920 to 2016, Agric. Water Manag., 237, 106195, https://doi.org/10.1016/j.agwat.2020.106195, 2020.

Kannenberg, S. A., Schwalm, C. R., and Anderegg, W. R. L.: Ghosts of the past: How drought legacy effects shape forest functioning and carbon cycling, Ecol. Lett., 23, 891–901, https://doi.org/10.1111/ele.13485, 2020.

Konduri, V. S., Morton, D. C., and Andela, N.: Tracking changes in vegetation structure following fire in the Cerrado biome using ICESat-2, J. Geophys. Res. Biogeosci., 128, e2022JG007046, https://doi.org/10.1029/2022JG007046, 2023.

Lawal, S., Hewitson, B., Egbebiyi, T. S., and Adesuyi, A.: On the suitability of using vegetation indices to monitor the response of Africa's terrestrial ecoregions to drought, Sci. Total Environ., 792, 148282, https://doi.org/10.1016/j.scitotenv.2021.148282, 2021.

Li, Y., Zhuang, J., Bai, P., Yu, W., Zhao, L., Huang, M., and Xing, Y.: Evaluation of three long-term remotely sensed precipitation estimates for meteorological drought monitoring over China, Remote Sens., 15, 154, https://doi.org/10.3390/rs15010086, 2023.

Narvaez, L., and Eberle, C.: Southern Madagascar food insecurity, Interconnected Disaster Risks, UNU-EHS Reports, 2021/2022, https://doi.org/10.53324/JVWR3574, 2022.

Lim Kam Sian, K. T., Zhi, X., Ayugi, B. O., Onyutha, C., Shilenje, Z. W., and Ongoma, V.: Meteorological drought variability over Africa from multisource datasets, Atmosphere, 14, 1052, https://doi.org/10.3390/atmos14061052, 2023.

Macron, C., Richard, Y., Garot, T., Bessafi, M., Pohl, B., Ratiarison, A., and Razafindrabe, A.: Intraseasonal rainfall variability over Madagascar, Mon. Weather Rev., 144, 1877–1885, https://doi.org/10.1175/MWR-D-15-0077.1, 2016.

McKee, T. B., Doesken, N. J., and Kleist, J.: The relationship of drought frequency and duration to time scales, in: Proceedings of the 8th Conference on Applied Climatology, Anaheim/Canada, 17–23 January, 179–184, 1993.

Mishra, A. K., and Singh, V. P.: A review of drought concepts, J. Hydrol., 391, 202–216, https://doi.org/10.1016/j.jhydrol.2010.07.012, 2010.

Masih, I., Maskey, S., Mussá, F. E. F., and Trambauer, P.: A review of droughts on the African continent: A geospatial and long-term perspective, Hydrol. Earth Syst. Sci., 18, 3635–3649, https://doi.org/10.5194/hess-18-3635-2014, 2014.

Nanzad, L., Zhang, J., Tuvdendorj, B., Nabil, M., Zhang, S., and Bai, Y.: NDVI anomaly for drought monitoring and its correlation with climate factors over Mongolia from 2000 to 2016, J. Arid Environ., 164, 69–77, https://doi.org/10.1016/j.jaridenv.2019.01.019, 2019.

Nguyễn, Q. T., Govind, A., Le, M. H., Nguyen, T. M. L., Linh, N. T. M., Anh, T. M. T., Hai, N. K., and Ha, T. V.: Spatiotemporal characterization of droughts and vegetation response in Northwest Africa from 1981 to 2020, Egyptian J. Remote Sens. Space Sci., https://doi.org/10.1016/j.ejrs.2023.05.006, 2023.

Nicholson, S. E., and Kim, J.: The relationship of the El Niño-Southern Oscillation to African Rainfall, Int. J. Climatol., 17, 117–135, https://doi.org/10.1002/(SICI)1097-0088(199702)17:2<117::AID-JOC84>3.0.CO;2-O, 1997.

Mbatha, N., and Sifiso, X.: Time series analysis of MODIS-derived NDVI for the Hluhluwe-Imfolozi Park, South Africa: Impact of recent intense drought, Climate, 6, 95, https://doi.org/10.3390/cli6040095, 2018.

Nkunzimana, A., Shuoben, B., Guojie, W., Alriah, M. A. A., Sarfo, I., Zhihui, X., Vuguziga, F., and Ayugi, B. O.: Assessment of drought events, their trend and teleconnection factors over Burundi, East Africa, Theor. Appl. Climatol., 145, 1293–1316, https://doi.org/10.1007/s00704-021-03680-3, 2021.

Nooni, I. K., Hagan, D. F. T., Wang, G., Ullah, W., Li, S., Lu, J., and Zhu, C.: Spatiotemporal characteristics and trend analysis of two evapotranspiration-based drought products and their mechanisms in sub-Saharan Africa, Remote Sens., 13, 533, https://doi.org/10.3390/rs13030533, 2021.

Rakhmatova, N., Arushanov, M., Shardakova, L., Nishonov, B., Taryannikova, R., Rakhmatova, V., and Belikov, D. A.: Evaluation of the perspective of ERA-Interim and ERA5 reanalyses for calculation of drought indicators for Uzbekistan, Atmosphere, 12, https://doi.org/10.3390/atmos12050527, 2021.

Randriamarolaza, L. Y. A., Aguilar, E., Skrynyk, O., Sergio, M., Vicente-Serrano, and Domínguez-Castro, F.: Indices for daily temperature and precipitation in Madagascar, based on quality-controlled and homogenized data, 1950-2018, Int. J. Climatol., 42, 265-288, https://doi.org/10.1002/joc.7243, 2021.

Randriatsara, H. H. -R. H., Hu, Z., Ayugi, B., Makula, E. K., Vuguziga, F., and Nkunzimana, A.: Interannual characteristics of rainfall over Madagascar and its relationship with the Indian Ocean sea surface temperature variation, Theor. Appl. Climatol., 148, 349–362, http://dx.doi.org/10.1007/s00704-022-03950-8, 2022a.

Randriatsara, H. H. -R. H., Hu, Z., Xu, X., Ayugi, B., Sian, K. T. C. L. K., Mumo, R., and Ongoma, V.: Evaluation of gridded precipitation datasets over Madagascar, Int. J. Climatol., 42, 7028–7046, http://dx.doi.org/10.1002/joc.7628, 2022b.

Randriatsara, H. H. -R. H., Hu, Z., Xu, X., Ayugi, B., Sian, K. T. C. L. K., Mumo, R., Ongoma, V., and Holtanova, E.: Performance evaluation of CMIP6 HighResMIP models in simulating precipitation over Madagascar, Int. J. Climatol., http://dx.doi.org/10.1002/joc.8153, 2023.

Randriatsara, H. H.-R. H., Holtanová, E., Rizwan, K., Babaousmail, H., Rabezanahary, M. F. T., Posset, K. R., Alupot, D., & Brian Odhiambo, A.: Historical changes in drought characteristics and its impact on vegetation cover over Madagascar [Data set]. Zenodo. https://doi.org/10.5281/zenodo.14844777, 2024.

Rigden, A., Golden, C., Chan, D., and Huybers, P.: Climate change linked to drought in Southern Madagascar, Clim. Atmos. Sci., 7, 41, https://doi.org/10.1038/s41612-024-00583-8, 2024.

Shalishe, A., Bhowmick, A., and Elias, K.: Meteorological drought monitoring based on satellite CHIRPS product over Gamo Zone, Southern Ethiopia, Adv. Meteorol., 2022, 1–13, https://doi.org/10.1155/2022/9323263, 2022.

Sharma, M., Bangotra, P., Gautam, A. S., and Gautam, S.: Sensitivity of normalized difference vegetation index (NDVI) to land surface temperature, soil moisture and precipitation over district Gautam Buddh Nagar, UP, India, Stoch. Environ. Res. Risk Assess., 36, 1779–1789, https://doi.org/10.1007/s00477-021-02066-1, 2022.

Sheffield, J., Wood, E. F., and Roderick, M. L.: Little change in global drought over the past 60 years, Nature, 491, 435–438, https://doi.org/10.1038/nature11575, 2012.

Smit, H. J., Metzger, M. J., and Ewert, F.: Spatial distribution of grassland productivity and land use in Europe, Agric. Syst., 98, 208–219, https://doi.org/10.1016/j.agsy.2008.07.004, 2008.

Rouse, J.W., Haas, R.H., Schell, J.A., & Deering, D.W. (1974). "Monitoring Vegetation Systems in the Great Plains with ERTS." Proceedings of the Third Earth Resources Technology Satellite-1 Symposium, Volume 1, pp. 309-317, https://ntrs.nasa.gov/citations/19740022614, 1974.

Staten, P. W., et al.: Tropical widening: From global variations to regional impacts, Bull. Am. Meteorol. Soc., 101, E897–E904, https://doi.org/10.1175/BAMS-D-19-0047.1, 2020.

Sun, J., Wang, X., Chen, A., Ma, Y., Cui, M., and Shilong, P.: NDVI indicated characteristics of vegetation cover change in China's metropolises over the last three decades, Environ. Monit. Assess., 179, 1–14, http://dx.doi.org/10.1007/s10661-010-1715-x, 2011.

Svoboda, M. D., and Fuchs, B. A.: Handbook of drought indicators and indices, Drought Water Crises: Integrating Science, Management, and Policy, 155–208, https://doi.org/10.9781351967525, 2017.

Tall, M., Sylla, M. B., Dajuma, A., Almazroui, M., Houteta, D. N. K., Klutse, N. A. B., Dosio, A., Lennard, C., Driouech, F., Diedhiou, A., and Giorgi, F.: Drought variability, changes and hot spots across the African continent during the historical period (1928–2017), Int. J. Climatol., 43, 7795–7818, https://doi.org/10.1002/joc.8293, 2023.

Tian, F., Fensholt, R., Verbesselt, J., Grogan, K., Horion, S., and Wang, Y.: Evaluating temporal consistency of long-term global NDVI datasets for trend analysis, Remote Sens. Environ., 163, 326–340, https://doi.org/10.1016/j.rse.2015.03.014, 2015.

Tladi, T. M., Ndambuki, J. M., and Salim, R. W.: Meteorological drought monitoring in the Upper Olifants sub-basin, South Africa, Phys. Chem. Earth, 128, 103273, https://doi.org/10.1016/j.pce.2022.103273, 2022.

The NCAR Command Language (Version 6.6.2) Software: Boulder, Colorado: UCAR/NCAR/CISL/TDD, https://www.ncl.ucar.edu/Applications/spi.shtml. Last access: 11 June 2023.

Thom, H. C. S.: A note on the gamma distribution, Mon. Weather Rev., 86, 117–122, https://doi.org/10.1175/1520-0493(1958)086<0117:ANOTGD>2.0.CO;2, 1958.

Udmale, P., Ichikawa, Y., Manandhar, S., Ishidaira, H., and Kiem, A.: Farmers' perception of drought impacts, local adaptation and administrative mitigation measures in Maharashtra State, India, Int. J. Disaster Risk Sci., 10, 250–269, https://doi.org/10.1016/j.ijdrr.2014.09.011, 2014.

Vicente-Serrano, S. M., Domínguez-Castro, F., Reig, F., Tomas-Burguera, M., Peña-Angulo, D., Latorre, B., Beguería, S., Rabanaque, I., Noguera, I., Lorenzo-Lacruz, J., and El Kenawy, A.: A global drought monitoring system and dataset based on ERA5 reanalysis: A focus on crop-growing regions, Geosci. Data J., https://doi.org/10.1002/gdj3.178, 2022.

Vicente-Serrano, S. M., Gouveia, C., Camarero, J. J., Beguería, S., Trigo, R., López-Moreno, J. I., Azorín-Molina, C., Pasho, E., Lorenzo-Lacruz, J., Revuelto, J., Sanchez-Lorenzo, A., Garcia-Cediel, E., Ramos, P., and Lamela, M.: Response of vegetation to drought time-scales across global land biomes, Proc. Natl. Acad. Sci. U. S. A., 110, 52–57, https://doi.org/10.1073/pnas.1207068110, 2013.

Wilhite, D. A.: Drought as a natural hazard: Concepts and definitions. In Drought, A Global Assessment; Ed.; Routledge: London, UK, Volume I, pp. 3–18, https://doi.org/10.4324/9781315830896, 2000.

Wilks, D. S.: Statistical Methods in the Atmospheric Sciences, volume 91 of International Geophysics Series, Academic Press, Burlington, USA, 627 pp., ISBN: 0127519661, 2005.

Wright, J. S., Fu, R., Worden, J. R., Chakraborty, S., Clinton, N. E., Risi, C., Sun, Y., and Yin, L.: Rainforest-initiated wet season onset over the southern Amazon, *Proc. Natl. Acad. Sci.*, 114, 8481–8486, https://doi.org/10.1073/pnas.1621516114, 2017.

Xian, T., Xia, J., Wei, W., Zhang, Z.,Wang, R., Wang, L. P.,Ma, Y. F.: Is Hadley Cell expanding?, Atmosphere, 12, 1699, https://doi.org/10.3390/atmos12121699, 2021.

Yao, N., Li, Y., Lei, T., and Peng, L.: Drought evolution, severity and trends in mainland China over 1961–2013, Science of The Total Environment, 616-617, 73–89, https://doi.org/10.1016/j.scitotenv.2017.10.327, 2018.

Zhang, M., Wang, K., Liu, H., Yue, Y., Ren, Y., Chen, Y., Zhang, C., Deng, Z.: Vegetation inter-annual variation responses to climate variation in different geomorphic zones of the Yangtze River Basin, China, Ecological Indicators, 152, 110357, https://doi.org/10.1016/j.ecolind.2023.110357, 2023.

Zhao, Z., Zhang, Y., Liu, L. S., and Hu, Z.: The impact of drought on vegetation conditions within the Damqu River Basin, Yangtze River Source Region, China, PLoS One, 13(8):e0202966, https://doi.org/10.1371/journal.pone.0202966, 2018.